

MAGNETIC SPECTROSCOPY OF NiO THIN FILMS AT THE OXYGEN K-EDGE USING THE PLS-II 2A BEAMLINE*

Y. Park[†], POSTECH, Pohang, Korea

Abstract

We performed magnetic spectroscopy experiments at the PLS-II 2A beamline to investigate the element-specific magnetic properties of NiO thin films. X-ray absorption spectroscopy (XAS) at the oxygen K-edge was used to probe the electronic structure of oxygen, while X-ray magnetic circular dichroism (XMCD) at the nickel L-edge revealed the spin and orbital magnetic moments of nickel. The XMCD signal observed at the oxygen edge further suggests induced magnetism in oxygen atoms through hybridization and magnetic exchange with adjacent nickel atoms. These results offer insight into interfacial magnetic coupling in transition metal oxides.

INTRODUCTION

XAS is a widely used technique for investigating the unoccupied electronic states and local chemical environment of specific elements. It provides element-specific information by measuring the absorption of X-rays as the photon energy is scanned across core-level binding energies. In transition metal oxides, XAS at the *K*- or *L*-edges reveals insights into the *p*- and *d*-orbital character and oxidation states of the constituent elements.

XMCD, obtained as the difference between XAS spectra recorded with left- and right-circularly polarized X-rays under an applied magnetic field, enables the study of element-specific magnetic properties. The dichroic signal reflects the spin and orbital contributions to the magnetic moment, making XMCD a powerful probe of magnetic ordering, spin polarization, and exchange interactions in complex materials.

In this study, we investigate the magnetic response of NiO using XAS and XMCD. The following section provides a brief overview of the fundamental principles underlying these spectroscopic techniques.

BASIC THEORY

XAS

XAS measures how the absorption of X-rays by a material varies as a function of photon energy. When the incident photon energy E matches the energy difference between a core level and unoccupied states, X-ray absorption increases sharply, leading to the appearance of characteristic absorption edges.

The degree of absorption at a given energy is described by the linear absorption coefficient $\mu(E)$. As X-rays pass

through a sample of thickness t , the transmitted intensity I_t follows the Beer–Lambert law:

$$I_t = I_0 \exp[-\mu(E)t], \quad (1)$$

where I_0 is the incident intensity. Figure 1 illustrates the basic physical principles underlying XAS.

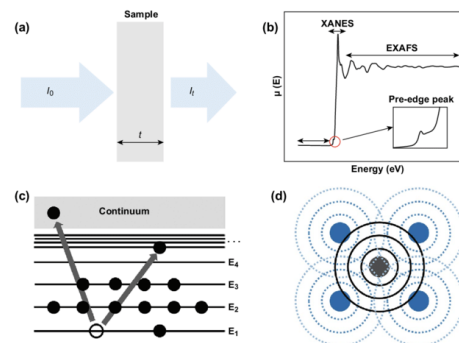


Figure 1: (a) Exponential attenuation of X-ray intensity as it passes through the sample. (b) Representative XAS spectrum, showing the X-ray Absorption Near Edge Structure (XANES) and Extended X-ray Absorption Fine Structure (EXAFS) regions as a function of photon energy. (c) Schematic of an X-ray-induced electronic transition from a core level to unoccupied states. (d) Interference pattern created by the outgoing (solid black lines) and reflected (dashed blue lines) photoelectron waves between the absorbing atom (gray) and its nearest neighbors (purple) [1].

XAS spectra can be recorded using various detection modes, depending on the sample characteristics and experimental objectives. Total electron yield (TEY) detects the number of secondary electrons emitted from the surface and provides high surface sensitivity, typically within a few nanometers. Fluorescence yield (FY), on the other hand, collects X-ray fluorescence photons emitted during core-hole relaxation and is more bulk-sensitive, with a probing depth extending to hundreds of nanometers, though it may suffer from self-absorption effects.

Partial electron yield (PEY) improves signal quality by selecting electrons within a specific kinetic energy range, reducing background noise from low-energy secondaries and offering a balance between sensitivity and spectral resolution. Transmission yield (TY) directly measures the X-ray intensity transmitted through the sample, yielding the most accurate determination of the absorption coefficient $\mu(E)$, but it requires sufficiently thin samples to allow measurable transmission.

* WORK SUPPORTED BY POHANG ACCELERATOR LABORATORY (PAL).

[†] pym102048@postech.ac.kr

XMCD

X-rays behave as transverse electromagnetic waves in vacuum or uniform, isotropic media, where the electric and magnetic fields oscillate perpendicular to the direction of propagation. Their polarization is defined by the phase relationship between the electric field components in the x - and y -directions. When these components are in phase or out of phase by π , the wave is linearly polarized; when they differ by $\pm\pi/2$, the wave becomes circularly polarized (left or right). In circularly polarized light, the electric field vector rotates in the transverse plane as the wave propagates.

The absorption of circularly polarized X-rays by a magnetic material depends on the relative orientation between the photon helicity and the sample's magnetization. This leads to a difference in absorption for left- and right-circularly polarized light, known as XMCD. XMCD originates from the spin-dependent transition probabilities due to exchange-split core and valence states, and thus provides element- and orbital-specific magnetic information.

X-ray Magnetic Circular Dichroism (XMCD) spectra allow quantitative extraction of magnetic moments using sum rules. The orbital and spin magnetic moments can be obtained through integrals over the dichroic ($\mu^+ - \mu^-$) and total ($\mu^+ + \mu^-$) absorption spectra.

The orbital magnetic moment is given by

$$m_{\text{orb}} = - \frac{4 \int_{L_3+L_2} (\mu^+ - \mu^-) d\omega}{3 \int_{L_3+L_2} (\mu^+ + \mu^-) d\omega} \cdot (10 - n_{3d}). \quad (2)$$

The spin magnetic moment is expressed as

$$m_{\text{spin}} = - \frac{6 \int_{L_3} (\mu^+ - \mu^-) d\omega - 4 \int_{L_3+L_2} (\mu^+ - \mu^-) d\omega}{\int_{L_3+L_2} (\mu^+ + \mu^-) d\omega} \cdot (10 - n_{3d}) \cdot \left(1 + \frac{7\langle T_z \rangle}{2\langle S_z \rangle}\right)^{-1}, \quad (3)$$

Those expressions were derived by Thole and Carra *et al.* [2, 3].

In these expressions, μ^+ and μ^- are the absorption coefficients for right and left circularly polarized light, respectively. The integrals are taken over the L_3 and L_2 absorption edges. n_{3d} is the number of 3d electrons in the absorbing atom. The term $\langle T_z \rangle$ denotes the magnetic dipole operator, and $\langle S_z \rangle$ is the expectation value of the spin angular momentum.

To observe XMCD, it is necessary to distinguish the absorption of right and left circularly polarized x-rays. While this can be achieved by switching the polarization of the incident x-ray beam, an equivalent effect can also be obtained by reversing the direction of the applied magnetic field, due to the time-reversal symmetry of the magnetic interaction.

XAS AND XMCD MEASUREMENTS AT PLS-II 2A BEAMLINE

PLS-II 2A Beamline

XAS and XMCD measurements were conducted at the 2A beamline of the PLS-II synchrotron radiation facility. The optical schematic of the beamline is shown in Fig. 2.

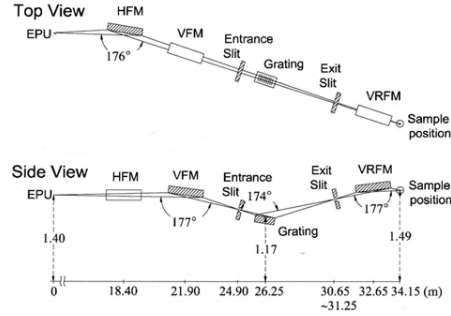


Figure 2: Schematic of the PLS-II 2A beamline for XAS and XMCD measurements. (top) Top view of the beamline layout (bottom) Side view of the beamline layout.

The beam is generated by an Elliptically Polarizing Undulator (EPU), which provides soft x-rays with tunable polarization. By adjusting the phase or varying the gap of the EPU, both the polarization state (linear or circular) and photon energy of the emitted beam can be finely controlled.

The beam then passes through a grating and a series of focusing optics before reaching the sample position, where XAS and XMCD spectra are collected.

The end station consists of four distinct sections, among which only the parts relevant to XAS and XMCD measurements are utilized in this study. The detailed layout of the end station is shown in Fig. 3.

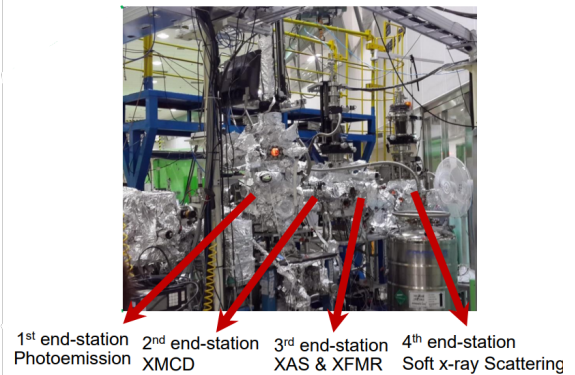


Figure 3: Configuration of the end station at the PLS-II 2A beamline. The system is divided into four sections, of which only the components related to XAS and XMCD measurements are used in this study.

During XAS and XMCD measurements, the sample was mounted as shown in Fig. 4, and its vertical position was



Figure 4: Schematic of the sample geometry used during XAS and XMCD measurements.

precisely controlled to ensure consistent energy-dependent scans.

XAS result

To identify the oxygen *K*-edge, X-ray absorption was scanned over the photon energy range of 500–560 eV. A pronounced absorption feature was observed near 530 eV, which corresponds to the transition from the O 1s core level to unoccupied 2*p* states. This feature is characteristic of the O *K*-edge and indicates strong hybridization with neighboring electronic states in the system, as shown in Fig. 5.

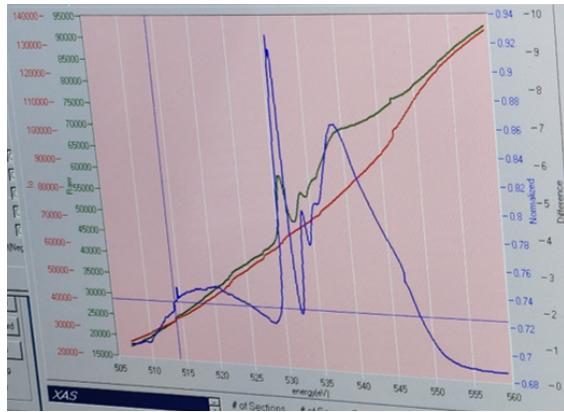


Figure 5: XAS spectrum of NiO measured in the 500–560 eV range, showing a distinct absorption peak at approximately 530 eV, corresponding to the O *K*-edge.

XMCD result

In the case of XMCD measurements, the photon energy was scanned from 840 to 885 eV to observe the Ni *L*-edge. As mentioned earlier, the XMCD signal was obtained by reversing the external magnetic field while maintaining a

fixed polarization state. The resulting spectrum exhibits a negative peak at the *L*₃ edge and a positive peak at the *L*₂ edge. These features arise from the spin-dependent absorption processes and reflect the spin and orbital magnetic moments of Ni, as described by the XMCD sum rules. The result is shown in Fig. 6.

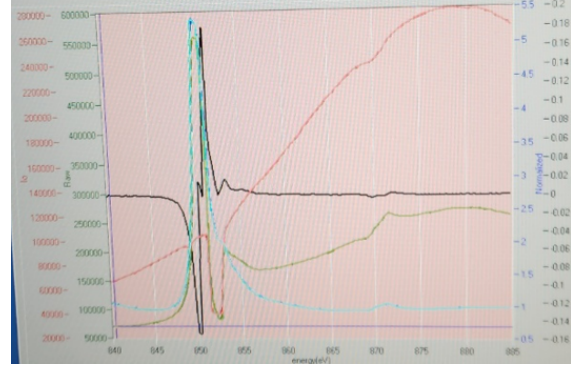


Figure 6: XMCD spectrum of Ni *L*-edge measured from 840 to 885 eV. A negative peak appears near 850 eV corresponding to the *L*₃ edge, and a positive peak near 853 eV corresponds to the *L*₂ edge.

CONCLUSION

We have conducted XAS and XMCD measurements at the PLS-II 2A beamline to investigate the element-specific magnetic properties of NiO thin films. The oxygen *K*-edge XAS spectrum revealed a strong absorption peak near 530 eV, corresponding to transitions from O 1s to unoccupied 2*p* states, indicating strong hybridization with surrounding electronic orbitals. XMCD measurements at the Ni *L*-edge showed characteristic negative and positive dichroic signals at the *L*₃ and *L*₂ edges, respectively, reflecting the spin-polarized electronic structure of nickel.

REFERENCES

- [1] M. Wang, L. Arnadottir, Z. Xu, and Z. Feng, “In situ x-ray absorption spectroscopy studies of nanoscale electrocatalysts,” *Nano-Micro Letters*, vol. 11, 12 2019.
- [2] B. T. Thole, P. Carra, F. Sette, and G. van der Laan, “X-ray circular dichroism as a probe of orbital magnetization,” *Phys. Rev. Lett.*, vol. 68, pp. 1943–1946, Mar 1992. [Online]. Available: <https://link.aps.org/doi/10.1103/PhysRevLett.68.1943>
- [3] P. Carra, B. T. Thole, M. Altarelli, and X. Wang, “X-ray circular dichroism and local magnetic fields,” *Phys. Rev. Lett.*, vol. 70, pp. 694–697, Feb 1993. [Online]. Available: <https://link.aps.org/doi/10.1103/PhysRevLett.70.694>